LETTERS
PUBLISHED ONLINE: 5 AUGUST 2012 | DOI: 10.1038/NGEO1538
nature geoscience

Two-phase growth of high topography in eastern Tibet during the Cenozoic

E. Wang[1]*, E. Kirby[2,3], K. P. Furlong[2], M. van Soest[4], G. Xu[5], X. Shi[2], P. J. J. Kamp[5] and K. V. Hodges[4]

High topography in eastern Tibet is thought to have formed when deep crust beneath the central Tibetan Plateau flowed towards the plateau margin, causing crustal thickening and surface uplift[1,2]. Rapid exhumation starting about 10–15 million years ago is inferred to mark the onset of surface uplift and fluvial incision[3–6]. Although geophysical data are consistent with weak crust capable of flow[7,8], it is unclear how the timing[9] and amount of deformation adjacent to the Sichuan Basin during the Cenozoic era can be explained in this way[10,11]. Here we use thermochronology to measure the cooling histories of rocks exposed in a section that stretches vertically over 3 km adjacent to the Sichuan Basin. Our thermal models of exhumation-driven cooling show that these rocks, and hence the plateau margin, were subject to slow, steady exhumation during early Cenozoic time, followed by two pulses of rapid exhumation, one beginning 30–25 million years ago and a second 10–15 million years ago that continues to present. Our findings imply that significant topographic relief existed adjacent to the Sichuan Basin before the Indo-Asian collision. Furthermore, the onset of Cenozoic mountain building probably pre-dated development of the weak lower crust, implying that early topography was instead formed during thickening of the upper crust along faults. We suggest that episodes of mountain building may reflect distinct geodynamic mechanisms of crustal thickening.

The evolution of topography throughout the Indo-Asian collision zone remains at the centre of debates over the links between plateau growth and the Asian monsoonal climate[12], as well as over the geodynamics of intracontinental deformation[8]. In eastern Tibet, the preservation of high-elevation, low-relief surfaces atop the surface of the Tibetan Plateau[13] and an abrupt increase in cooling rates along the deeply exhumed margin of the plateau during late Miocene time[3–6,14–17] (Fig. 1) have led to the suggestion that high elevations across much of eastern Tibet developed in the past 10–15 million years (Myr). This conclusion is central to two geodynamic inferences; first, that the synchrony of mountain building around the periphery of the Tibetan Plateau and regional changes in climate are the consequences of a fundamental change in lithospheric buoyancy beneath the plateau[12], and second, that late Miocene growth of eastern Tibet heralds the initial development of a weak lower crust beneath the plateau[8].

Both of these hypotheses have been challenged recently. Isotopic data from central Tibet[18,19] suggest that thickened crust and high topography were established early in the collision history. This is consistent with slow erosion rates across the plateau in the past

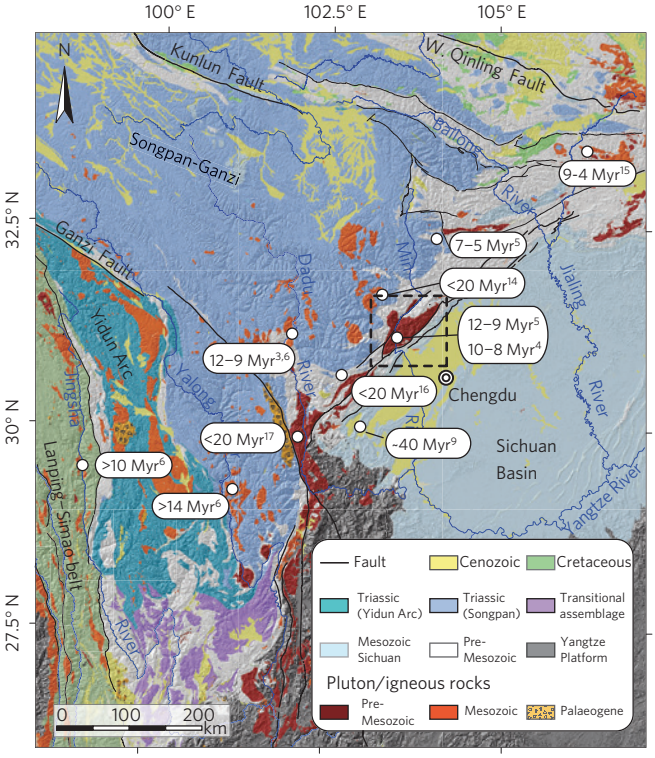

Figure 1 | Simplified regional geologic map of the eastern margin of the Tibetan Plateau. Tectonostratigraphic terranes are shown in the explanation. Estimates for the onset of rapid cooling based on thermochronologic data are given in Myr before present and are referenced in citations. Dashed box shows location of Fig. 2.

40 Myr (ref. 20) and with the preservation of relict plateau surfaces in the western Himalaya[21]. In northern Tibet, evidence for both deformation[22] and the establishment of high elevations[23] by Eocene time are likewise consistent with the expansion of a broad region of high topography in the Early Tertiary period. The eastern extent of such a proto-plateau, however, remains uncertain.

In eastern Tibet, the role of lower crustal flow in the development of high topography has been questioned in the Longmen Shan (Dragon's Gate Mountains), adjacent to the Sichuan Basin. Here, Cenozoic shortening[11,24] along an imbricate fan of basement-involved thrust faults has been argued to be primarily responsible

[1]State Key Laboratory of Lithospheric Evolution, Institute of Geology and Geophysics, Chinese Academy of Sciences, Beijing 10029, China, [2]Department of Geosciences, Penn State University, Pennsylvania 16802, USA, [3]Department of Earth and Environmental Sciences, Universität Potsdam, Potsdam 14476, Germany, [4]School of Earth and Space Exploration, Arizona State University, Arizona 85287, USA, [5]Department of Earth and Ocean Sciences, University of Waikato, Hamilton 3240, New Zealand. *e-mail: erchie-wang@mail.iggcas.ac.cn.

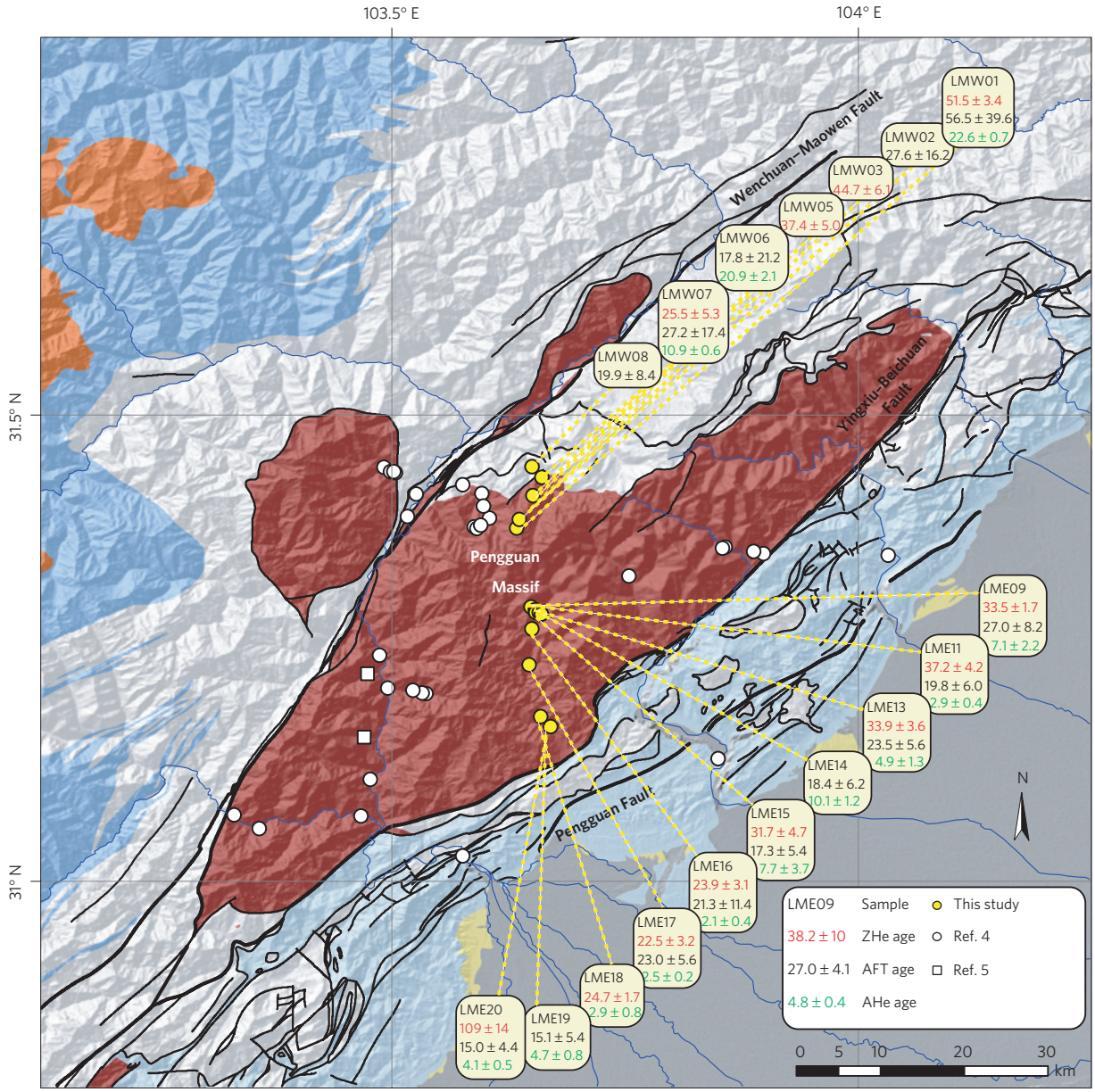

Figure 2 | Geologic map of the southern Longmen Shan range. Sample locations along an elevation transect (yellow) were sampled in the Pengguan Massif, a crystalline massif in the hanging wall of the Yingxiu–Beichuan Fault zone. Data from previous studies are available in the Supplementary Information. Explanation of geologic units as in Fig. 1.

for high topography and thickened crust[10]. Four primary fault systems seem to have accommodated Cenozoic deformation (Fig. 2): first, the Wenchuan–Maowen Fault, a steep to subvertical structure along the western flank of the Pengguan Massif; second, the Yingxiu–Beichuan Fault, a steep to moderately dipping reverse fault that places crystalline basement of the Pengguan Massif against Triassic rocks of passive margin affinity; third, the Pengguan Fault, a splay fault that forms the range front along the Longmen Shan; and fourth, an unnamed, blind structure beneath the Sichuan Basin[10,11,24]. Both the Yingxiu–Beichuan and the Pengguan faults are active and experienced relatively large displacements during the 2008 M_w 7.9 Wenchuan earthquake[25]. Because these structures have significant Mesozoic displacement[24], assessing the amount of shortening that accumulated during Cenozoic mountain building is challenging.

The timing of deformation and relief generation along the Longmen Shan is likewise uncertain. Cooling ages from the crystalline massifs in the range (Fig. 1) imply significant exhumation since about 10–15 Myr ago[4,5,14]. Slow cooling before this time is argued to reflect little to no topographic relief between the range and its foreland[5]. However, thermally reset apatite-fission-track ages from the Xiongpo anticline, a fault-related fold in the southwestern Sichuan Basin (Fig. 1), suggest exhumation about 40 Myr ago[9]. Structural relationships between a belt of klippen that lie to the east of the basement massifs and folded Cretaceous—Eocene strata in the Sichuan Basin (Fig. 2) suggest the emplacement of the klippen since Eocene time[24]. Thus, geologic data permit the possibility that deformation began as early as the mid-Cenozoic era[26].

To assess the timing and history of mountain building in the Longmen Shan, we present new thermochronologic data from a densely sampled ($n = 20$) age–elevation transect in the Pengguan Massif, adjacent to the Sichuan Basin (Fig. 1). The transect spans nearly 3 km of relief and is located in the immediate hanging wall of the Yingxiu–Beichuan Fault, the primary structure responsible for

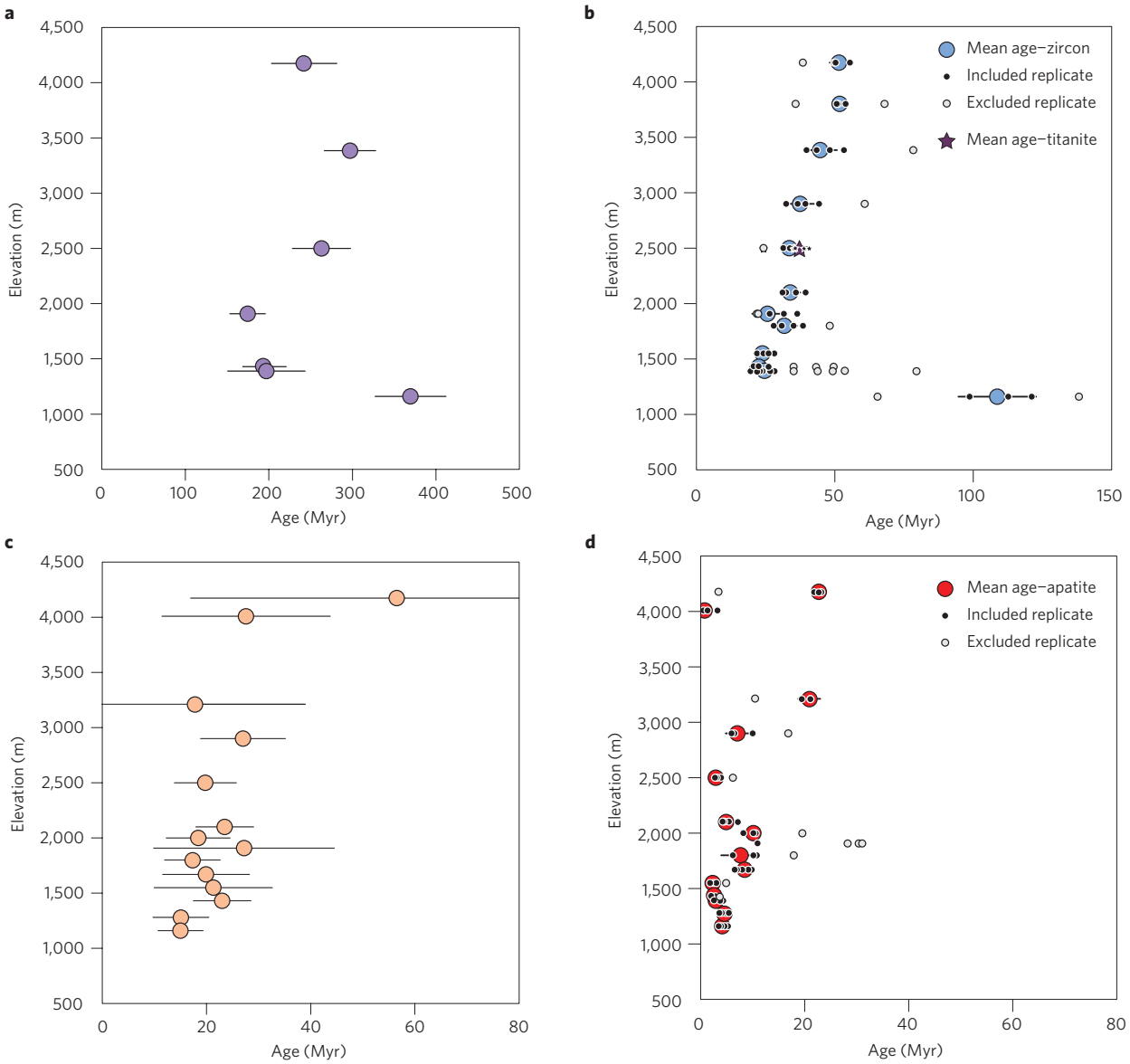

Figure 3 | Age–elevation relationships for thermochronologic data from the Pengguan Massif. 2σ analytical uncertainties are shown as error bars. **a**, ZFT determinations. **b**, ZHe ages (circles) and titanite (U–Th)/He ages (star). Filld symbols denote grain replicates included in the mean age determination. Open symbols denote excluded grain ages. **c**, AFT ages. **d**, AHe ages. Symbols as in **b**.

the M_w 7.9 2008 Wenchuan earthquake[25]. Thus, the exhumational history of this portion of the range provides an important constraint on the history of slip along this fault system[4]. We present results from numerous thermochronologic systems, including (U–Th)/He in apatite (AHe) and zircon (ZHe) and fission track in apatite (AFT) and zircon (ZFT) in Fig. 3 and Supplementary Tables S5–S9. Together, the kinetics of He diffusion and fission-track annealing in these systems span a temperature window ranging from ~250–300 °C down to ~60 °C (ref. 27) and allow us to interrogate the thermal history of this part of the plateau margin in unprecedented detail.

Results from ZFT analysis of seven samples yield ages that range from about 200 to 250 Myr (Fig. 3a), implying that rocks now at the surface resided at or above ~250 °C during the early Cenozoic[27]. These results place a maximum bound on total exhumation of ~10–12 km (see Supplementary Information). In contrast, ZHe ages from 12 samples vary systematically with elevation (Fig. 3b), ranging from 51.5 ± 3.4 at ~4,200 m to 24.7 ± 1.7 at ~1,400 m elevation (all uncertainties are quoted at two standard deviations (σ)). Although generally older than previous ZHe determinations from this massif[4], our results are confirmed by numerous replicates of individual grains (Supplementary Table S7) and by analyses of titanite from a single sample (Fig. 3b). These results imply cooling through ~180 °C (ref. 27) during the early and mid-Cenozoic.

Ages from AFT and AHe thermochronologic systems provide additional insight into the late Cenozoic cooling history. AFT ages range from 27.6 ± 16.2 Myr at ~4,000 m to 15.0 ± 4.4 Myr at the base of the transect (Fig. 3c), but most ages are relatively invariant with elevation about 25 Myr ago (Fig. 3c). Relatively long confined track lengths in these samples (Supplementary Fig. S2) are consistent with a period of increased cooling rate during this time interval. AHe ages are generally young in the lower half of the transect (Fig. 3d), ranging in age from 10.9 ± 0.6 Myr at ~1,900 m to 4.1 ± 0.5 Myr at ~1,160 m. AHe ages above 1,900 m elevation are sparse, owing to poor-quality apatites (see Supplementary Information), but two well-determined results yield ages of about 22–23 Myr.

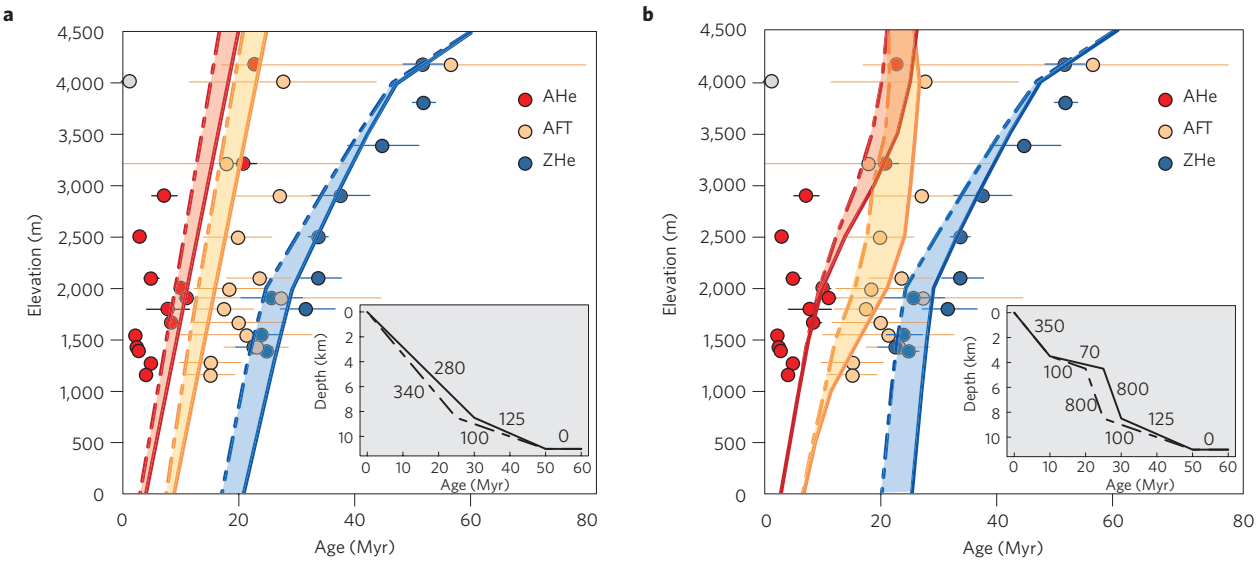

Figure 4 | Composite age–elevation transect comparing data with predictions of thermal models. Uncertainties are shown as 2σ. Insets show time-depth histories of samples exposed at the surface at present used in forward models. Numbers represent average exhumation rates in m Myr^{-1} for each stage. **a**, Single-stage exhumation histories that represent acceleration starting 30 Myr (solid lines) or 25 Myr ago (dashed lines). Shaded region between two histories represents range of solutions between these time periods. **b**, Two-stage thermal histories consistent with the ensemble of low-temperature thermochonometers. Onset of rapid exhumation 30 Myr (solid lines) or 25 Myr ago (dashed lines) is followed by a period of slow exhumation (inset). Rapid exhumation commencing 10 Myr ago is common to both histories.

These results clearly reveal a protracted history of exhumation along the Longmen Shan and challenge the interpretation that topographic relief along this margin of the plateau developed entirely in the late Miocene[4,5]. Although the duration and extent of exhumation recorded by our data preclude preservation of abrupt changes in the slope of age–elevation arrays of any single system[3], thermal modelling of exhumation histories consistent with the suite of thermochronologic data require protracted, but episodic, exhumation.

First, some topographic relief clearly existed along the Longmen Shan during the Early Tertiary period. A linear fit to the age–elevation trend of ZHe results suggests exhumation at rates of ~90–100 m Myr^{-1} during the interval 50–30 Myr ago (Supplementary Fig. S3). A simple analysis of scaling relationships between the relief along actively incising river profiles and modern erosion rates from eastern Tibet[28,29] demonstrates that sustained, slow denudation rates were probably associated with relatively low relief across the Longmen Shan in the Early Tertiary. Our analysis follows a broad body of work that demonstrates that channel steepness (a measure of channel gradient normalized for differences in basin shape) is correlated with erosion rate. In modern-day eastern Tibet, erosion rates of ~100 m Myr^{-1} are associated with relatively low-gradient channels (channel steepness indices of ~50–100 m$^{0.9}$; ref. 29). Assuming that channels were of similar length to today (a conservative minimum, see Supplementary Information), the difference in elevation across the Longmen Shan was probably no greater than ~750–1,000 m (Supplementary Fig. S4), implying that $\gtrsim$75% of the present-day relief between the plateau and the Sichuan Basin (~4,000 m) developed during the Cenozoic.

Second, thermal histories imply that exhumation rates must have increased in the late Oligocene–early Miocene. This result is required by the steep age–elevation trend of the AFT data, by the convergence of ZHe and AFT ages near the base of the transect (Fig. 4) and by AFT lengths (Supplementary Fig. S2). Although our data do not distinguish whether the onset of accelerated exhumation occurred 30 or 25 Myr ago (Fig. 4), it is clear that rapid exhumation (~1,000 m Myr^{-1}) was ongoing during the early Miocene. Thus, our results directly contradict previous studies[4,5] that infer slow cooling during the mid-Cenozoic and imply that substantial relief along the present-day margin of eastern Tibet had begun to develop by Oligocene–Miocene time.

Third, our results require temporally unsteady exhumation during the mid-to-late Cenozoic. A key result is the presence of AHe ages of about 20 Myr at the top of the range, which demand a hiatus or decrease in exhumation rate during the mid-Miocene (about 20–10 Myr ago, Fig. 3). Although the duration of this period is not well resolved, models that maintain steady rates of exhumation from the Oligocene to the present day systematically misfit both the AFT and AHe data (Fig. 4a). However, all models also indicate that this hiatus must have been followed by a second period of rapid exhumation in the past ~10 Myr (as argued previously[4,5]), such that relatively young AHe ages (about 4 Myr) are present in the lower half of the transect (Fig. 3d).

This episodic history of exhumation challenges much present thinking about the timing and processes responsible for the generation of high topography along the eastern margin of the Tibetan Plateau. Our results reveal a previously unrecognized pulse of mountain building adjacent to the Sichuan Basin in Oligocene time. Deformation at this time is recognized to the south and west of the Longmen Shan[8,26], but the relative contribution to plateau development remains uncertain. Our results suggest that shortening along structures in the Longmen Shan foreland[10] and emplacement of klippen was associated in time with significant exhumation of basement massifs in the core of the range. Thus, crustal thickening during this early period of deformation and exhumation represents a significant, if as yet unquantified, contribution to present-day topography.

This conclusion also raises the possibility that previous estimates of the timing of surface uplift in southeastern Tibet[3,6] may be incorrect. These studies implicitly assume a nearly instantaneous response of fluvial incision to surface uplift, but lags in the response time of erosional systems[30] make this inference subject to uncertainty. Moreover, isolated data from some regions of eastern Tibet suggest that the onset of rapid cooling pre-dates ~14 Myr (refs 6,17) and hints at the likelihood of earlier periods of exhumation. Our results raise the possibil-

ity that Oligocene–Miocene mountain building may have been widespread along the eastern plateau margin and that large regions of eastern Tibet may have attained significant elevation before the late Miocene[9].

Our findings carry important implications for the geodynamics of plateau formation in eastern Tibet. Notably, significant crustal thickening along the margin of the Sichuan Basin in Oligocene time cannot be readily attributed to the flow of lower crust. The timescales required for thermal weakening of the thickened crust to attain effective viscosities permissible of widespread flow are of the order of ~20 Myr (ref. 31). Even allowing for reasonable propagation velocities of a tunnelling channel[32], the onset of mountain building in eastern Tibet seems to be too close in time to the Indo-Asia collision for this process to be active.

Renewed exhumation in the Longmen Shan during the late Miocene, however, may still reflect thickening of the lower crust[8]. Although we cannot definitively rule out a role for climatically enhanced incision, the sustained exhumation required by our data from about 10 Myr ago to present (Fig. 4) and the widespread onset of exhumation at this time (Fig. 1) suggest an underlying tectonic driver. Late-Miocene plateau growth during the emplacement of weak lower crust is consistent with timescales of crustal flow[31,32]. We suggest that the onset of exhumation across eastern Tibet in the late Miocene probably reflects a fundamental shift in the dynamics of mountain building at this time such that plateau growth subsumed pre-existing ranges in the Longmen Shan and elsewhere[24]. Regardless, modern plateau topography in eastern Tibet retains a palimpsest of early Cenozoic mountain building that may be revealed only through high-resolution thermochronologic records.

Methods

Apatite and zircon were extracted from rock samples and concentrated following standard density and magnetic separation procedures. Fission-track ages were determined at the University of Waikato, using the external detector method and a zeta calibration factor for Fish Canyon, Durango and Mt. Dromedary age standards for AFT ages. Samples were irradiated in the Forschungsreaktor Heinz Maier-Leibnitz II reactor in Munich, with nominal fluences of 1×10^{16} neutrons cm^{-2} for apatite and 2×10^{15} neutrons cm^{-2} for zircon. Neutron fluences were monitored using CN5 (apatite) and CN1 (zircon) dosimeter glass and mica detectors were etched in HF. All samples were measured by G. Xu. Confined track lengths in apatite were measured by digitizing track terminations using a projection tube and are estimated to have a precision of 0.2 μm.

Euhedral crystals of apatite and zircon were hand-picked on the basis of size and clarity for (U–Th)/He analysis at the Arizona State University (ASU) and measured using digital images taken under ×184 magnification and dark-field illumination using a Leica MZ16 binocular microscope. Individual grains were loaded into Nb tubes and analysed for He on an Australian Scientific Instruments Alphachron (U–Th)/He system. He was released from each crystal by heating using a 980 nm diode laser and the gas was spiked with 3He, gettered to remove impurities and measured on a Pfeiffer-Balzers Prisma Quadrupole mass spectrometer. Average blank at ASU is 0.036 ± 0.013 (1σ) fmol. ^{4}He concentrations were calculated by comparison to a spiked ^{4}He standard (known to ± 1.2%) analysis run in sequence with the unknowns. All samples were subjected to re-extraction to ensure complete gas removal and grains were subsequently subjected to digestion for U and Th measurement. Details of the digestion procedures are available in the Supplementary Information. Solutions were spiked with ^{230}Th and ^{235}U and analysed on a Thermo X series quadrupole inductively coupled plasma mass spectrometer at ASU, using a micromettreebulizer. Finally, individual grain ages were calculated using blank-corrected values and corrected for a-ejection effects. Shards of Durango apatite, euhedral zircon crystals of Fish Canyon Tuff and abraded shards of titanite from Fish Canyon Tuff were analysed with the samples as age standards. Mean values of individual grain replicates were determined using a subset ($n > 3$, in all cases) of grain ages and propagating all uncertainties. A complete discussion of analytical procedures can be found in the Supplementary Information.

Forward models of the thermal response to exhumation were conducted using a one-dimensional finite-difference approximation to the advection–diffusion equation. Various exhumation histories were imposed subject to the constraint that total exhumation ranges between 10 and 12 km, using a constant initial surface heat flow of 75 mW m^{-2}, thermal conductivity of the crystalline basement of 3 W m^{-1} K^{-1}, surface radiogenic heat production of 2 μW m^{-3} (with an exponential scaling length of 10 km) and subject to a constant surface temperature of 0 °C. Comparison of these thermal histories with thermochronologic data was accomplished through modelling codes that track the radiogenic production and diffusion of He in apatite and the annealing of AFT. As the kinetics of diffusive loss of He from zircon are not completely understood, we simply track the 180 °C isotherm as a proxy for the closure temperature of this system. A full discussion of model parameters and sensitivity can be found in the Supplementary Information.

Received 16 January 2012; accepted 5 July 2012; published online 5 August 2012

References

1. Clark, M. K. & Royden, L. H. Topographic ooze: Building the eastern margin of Tibet by lower crustal flow. *Geology* **28,** 703–706 (2000).
2. Royden, L. H. *et al.* Surface deformation and lower crustal flow in Eastern Tibet. *Science* **276,** 788–790 (1997).
3. Clark, M. K. *et al.* Late Cenozoic uplift of southeastern Tibet. *Geology* **33,** 525–529 (2005).
4. Godard, V. *et al.* Late Cenozoic evolution of the central Longmen Shan, eastern Tibet: Insight from (U–Th)/He thermochronmetry. *Tectonics* **28,** TC5009 (2009).
5. Kirby, E. *et al.* Late Cenozoic uplift and landscape evolution along the eastern margin of the Tibetan Plateau: Inferences from ^{40}Ar/^{39}Ar and (U–Th)/He thermochronology. *Tectonics* **21,** TC1246 (2002).
6. Ouimet, W. *et al.* Regional incision of the eastern margin of the Tibetan Plateau. *Lithosphere* **2,** 50–63 (2010).
7. Bai, D. *et al.* Crustal deformation of the eastern Tibetan plateau revealed by magnetotelluric imaging. *Nature Geosci.* **3,** 358–362 (2010).
8. Royden, L. H., Burchfiel, B. C. & van der Hilst, R. D. The geological evolution of the Tibetan Plateau. *Science* **321,** 1054–1058 (2008).
9. Richardson, N. J. *et al.* Extraordinary denudation in the Sichuan Basin: Insights from low-temperature thermochronology adjacent to the eastern margin of the Tibetan Plateau. *J. Geophys. Res.* **113,** B04409 (2008).
10. Hubbard, J. & Shaw, J. H. Uplift of the Longmen Shan and Tibetan plateau, and the 2008 Wenchuan (m = 7.9) earthquake. *Nature* **458,** 194–197 (2009).
11. Jia, D. *et al.* Structural model of 2008 Mw 7.9 Wenchuan earthquake in the rejuvenated Longmen Shan thrust belt, China. *Tectonophysics* **491,** 174–184 (2010).
12. Molnar, P., Boos, W. R. & Battisti, D. S. Orographic controls on climate and paleoclimate of Asia: Thermal and mechanical roles for the Tibetan Plateau. *Annu. Rev. Earth Planet. Sci.* **38,** 77–102 (2010).
13. Clark, M. K. *et al.* Use of a regional, relict landscape to measure vertical deformation of the eastern Tibetan Plateau. *J. Geophys. Res.* **111,** F03002 (2006).
14. Arne, D. *et al.* Differential exhumation in response to episodic thrusting along the eastern margin of the Tibetan Plateau. *Tectonophysics* **280,** 239–256 (1997).
15. Enkelmann, E. *et al.* Cenozoic exhumation and deformation of northeastern Tibet and the Qinling: Is Tibetan lower crustal flow diverging around the Sichuan Basin? *Geol. Soc. Am. Bull.* **118,** 651–671 (2006).
16. Wilson, C. J. L. & Fowler, A. P. Denudational response to surface uplift in east Tibet: Evidence from apatite fission-track thermochronology. *Geol. Soc. Am. Bull.* **123,** 1966–1987 (2011).
17. Xu, G. & Kamp, P. Tectonics and denudation adjacent to the Xianshuihe Fault, eastern Tibetan Plateau: Constraints from fission track thermochronology. *J. Geophys. Res.* **105,** 19231–19251 (2000).
18. DeCelles, P. G. *et al.* High and dry in central Tibet during the Late Oligocene. *Earth Planet. Sci. Lett.* **253,** 389–401 (2007).
19. Rowley, D. B. & Currie, B. S. Paleo-altimetry of the late Eocene to Miocene Lunpola basin, central Tibet. *Nature* **439,** 677–681 (2006).
20. Rohrmann, A. *et al.* Thermochronologic evidence for plateau formation in central Tibet by 45 Ma. *Geology* **40,** 187–190 (2011).
21. van der Beek, P. *et al.* Eocene Tibetan plateau remnants preseved in the northwest Himalaya. *Nature Geosci.* **2,** 364–368 (2009).
22. Clark, M. K., Farley, K. A., Zheng, D., Wang, Z. & Duvall, A. R. Early Cenozoic faulting of the northern Tibetan Plateau margin from apatite (U–Th)/He ages. *Earth Planet. Sci. Lett.* **296,** 78–88 (2010).
23. Dupont-Nivet, G., Hoorn, C. & Konert, M. Tibetan uplift prior to the Eocene–Oligocene climate transition: Evidence from pollen analysis of the Xining Basin. *Geology* **36,** 987–990 (2008).
24. Burchfiel, B. C., Chen, Z., Liu, Y. & Royden, L. H. Tectonics of the Longmen Shan and adjacent regions. *Int. Geol. Rev.* **37,** 661–735 (1995).
25. Zhang, P-Z., Wen, X-Z., Shen, Z-K. & Chen, J-H. Oblique, high-angle, listric-reverse faulting and associated development of strain: The Wenchuan earthquake of May 12, 2008, Sichuan, China. *Annu. Rev. Earth Planet. Sci.* **38,** 351–380 (2010).
26. Tapponnier, P. *et al.* Oblique stepwise rise and growth of the Tibet Plateau. *Science* **294,** 1671–1677 (2001).

27. Reiners, P. W. & Brandon, M. T. Using thermochronology to understand orogenic erosion. *Annu. Rev. Earth Planet. Sci.* **34,** 419–466 (2006).
28. Ouimet, W. B., Whipple, K. X. & Granger, D. E. Beyond threshold hillslopes: Channel adjustment to base-level fall in tectonically active mountain ranges. *Geology* **37,** 579–582 (2009).
29. Kirby, E. & Ouimet, W. in *Growth and Collapse of the Tibetan Plateau* Vol. 353 (eds Gloaguen, R. & Ratschbacher, L.) 165–188 (Geological Society of London, 2011).
30. Craddock, W. H. *et al.* Rapid fluvial incision along the Yellow River during headward basin integration. *Nature Geosci.* **3,** 209–213 (2010).
31. Beaumont, C., Jamieson, R. A., Nguyen, M. H. & Medvedev, S. Crustal channel flows: 1. Numerical models with applications to the tectonics of the Himalayan-Tibetan orogen. *J. Geophys. Res.* **109,** B06406 (2004).
32. Medvedev, S. & Beaumont, C. in *Channel Flow, Ductile Extrusion and Exhumation in Continental Collision Zones* Vol. 268 (eds Law, R. D., Searle, M. P. & Godin, L.) 147–164 (Geological Society of London, 2006).

Acknowledgements

This project received financial support from Chinese National Key Projects (2011CB403106) and the National Natural Science Foundation of China (41130312, 40721003) to E.W. E.K. and K.P.F. were supported by the Tectonics program at NSF (EAR-0911587) and E.K. thanks the Alexander von Humboldt Foundation for support during the completion of this manuscript. We thank S. Zhe and X. Guang for assistance with sample collection.

Author contributions

E.W. conducted field work and collected samples. G.X. and P.J.J.K. were responsible for fission-track analyses and ages. M.v.S. and K.V.H. conducted (U–Th)/He analyses and age determination. K.P.F. carried out thermal modelling. E.W., E.K., K.P.F. and X.S. designed the study and wrote the manuscript; all authors discussed interpretations and commented on the manuscript.

Additional information

Supplementary information is available in the online version of the paper. Reprints and permissions information is available online at www.nature.com/reprints. Correspondence and requests for materials should be addressed to E.W.

Competing financial interests

The authors declare no competing financial interests.